EOS Space Systems wide field imager for SSA applications

Ian Ritchie
EOS Space Systems
Craig Smith
EOS Space Systems

Abstract:

EOS Space Systems (EOSSS) has designed and manufactured space surveillance imagers since 1999. From early adaptations of Celestron Nexstar™ tubes to use ICCD sensors, to current EMCCD sensors in custom designed optical assemblies, the company has been required to seek the widest fields possible on a systems small enough to ride on a larger telescope OTA. The latest 14 inch (350mm) variant uses f0.75 corrected optics to achieve real time (2 second) imaging to visual magnitude 16 or fainter, and fields of view up to 3 degrees given the appropriate image plane size. With mass of only 50 kg and up to 1 Mpix 14 bit sampling, this imager has many potential SSA applications.

Introduction

When observing space from the Earth, atmospheric seeing means that (without adaptive optics) most Earth orbiting objects are unresolved. For space surveillance operations, however, this allows us to optimise the design of imagers for the purposes of detection rather than recognition or resolved imaging of objects. This paper discusses the optimisations implied by this limitation, and the realisation of a wide field imager which is ideally suited to the detection and location needs of Space Situational Awareness observatories. The use of advanced sensor technologies, simplified optical design and stable lightweight materials may be combined to give fast operation at the practical limits of sensitivity. Objects down to 10cm in size can be detected in a few seconds using the EOS design, and the limitation is principally caused by star background rather than by the imager itself.

Practical Limitations in Wide Field Imaging

EOS Space Systems (EOS) has been developing wide field imaging sensors since its early laser ranging experiments with space debris in 2000. Prototype ICCD based imagers showed that the star field background creates confusion and can be a limitation on sensitivity, needing software algorithms to distinguish between targets and star streaks when satellite tracking. Early f2.0 prototype imaging systems were effective, but made from stainless steel they were impractical for easy use with 1m style telescopes. However, these early attempts in 2000 to 2003 showed the nature of the challenge quite clearly.

Accepting that seeing at available sites varies from sub arc second to >1.5 arc seconds, the ability to resolve shape was ignored in design specifications. Having recognized this fundamental issue, the issue of object recognition/ characterisation was diverted into the field of adaptive optics, and high speed imaging became an issue solely related to detection. This simplifies analysis to the point where calculation tools can be applied more readily.

Input values for yellow cells, green cells are calculated.					
Dataset 1		Data set 2		Seeing	
0.5	Wavelength of interest (microns)	4	Wavelength of interest (microns)	arc sec	
0.35	Mirror Diameter (m)	0.5	Mirror Diameter (m)	2	
0.75	f/#	4	f/#		
0.3	Total Circular Field Diameter (Deg)	1	Total Circular Field Diameter (Deg)		
12	Pixel side length (microns)	15	Pixel side length (microns)		
512	Number of pixels on a side	640	Number of pixels on a side		
0.92	microns Airy disc diameter	39.04	microns Airy disc diameter		
0.72	arc seconds Airy disc diameter	4.03	arc seconds Airy disc diameter		
9.43	arc seconds per pixel (side, not diagonal)	1.55	arc seconds per pixel (side, not diagonal)	1.3	Pixels per star rms diameter
0.79	arc seconds per micron	0.10	arc seconds per micron	1.3	Oversampling ratio for given seeing above
1.27	microns/arc second	9.70	microns/arc second		
0.11	Pixels per arc second				
1.37	Diameter of field in the image plane	34.91	Diameter of field in the image plane		
0.69	Radius in image plane	17.45	Radius in image plane		
4828	Arc seconds on CCD side	990	Arc seconds on CCD side		
1.34	Degrees on CCD side	0.28	Degrees on CCD side	990.1	arc seconds
13.11	Airy disc diameters per pixel	0.38	Airy disc diameters per pixel		
Note: IR Imager Sensitivity Chart uses dataset 1					
I:\GenericTools&Templates\OPTICS\[SSA Optical Systems Design Tool_ First Order Approximations_j .xls]AR Field Analyser					

Fig 1: Typical excel analysis tool for imager fields (courtesy Andrew Rakich 2003)

If we study the single issue of Field of View (FoV), then the two limiting factors in effectiveness are related to noise. At one extreme, narrow field sampling of the sky by digital imagers allows the image to fall onto many pixels, without achieving a practical benefit for recognition, as above: the signal is dissipated and the sensor noise limits sensitivity. At the opposite extreme in wide field sampling of the sky, there is the sky background noise per steradian, which limits sensitivity by washing out pixels with too much sky area, especially in moonlight conditions.

This leads us to an optimization zone where neither source of noise dominates. Matching the pixel size to the sky seeing limit is the solution to designing wide field imagers for tracking of objects. Now the major limitation is the quantum efficiency (QE) of the sensor. EOSSS began with ICCD style imagers, but the high voltage MCP style amplifiers were rejected as being too noisy, as well as being export restricted. Since 2004, EOSSS has employed EMCCD sensors on all detection imagers for the visible wavelength band. The only exceptional circumstance is that in the presence of pulsed lasers, ICCD type detectors may be electronically gated in the microsecond domain, which can save in filter design.

Imager Sensitivity Calculator

Data values in the blue cells come from data set #1 on the AR Field Analyser sheet, allowing the limiting Signal To Noise Ratio of an imager to be calculated for different star magnitudes
Update yellow cells only by hand for camera and site data, and the chart will show useful integration periods for the proposed system, for each visual magnitude

Mag 0 Power (w/sq cm/ um)	Telescope Aperture (m diameter)	Telescope Aperture (sq m)	Airy Disc Diameters Per Pixel	FoV arc seconds	FoV (mm)	Aperture Obscuration Ratio	Exposure Read Noise / pixel (eV)	Sensor mean QE over pass band	Sensor Bandpass (nm)	Pixel Max Well Depth	Site Mean Seeing (arc sec)	Sky Noise (ph/arc sec sq/ sec)	Imager Dark Current (ph/ sec)	Imager PE Gain		mag/ sq arcsec	Vm22.8	Vm20	Vm19
3.9E-12	0.35	0.096211	13.114754	4827.7751	1.3744499	0.1	12	0.62	500	1.00E+05	1.0	0.08	200	1000		ph/sq arcsec	0.08	1.29	3.22

Mag 0 Power (W/sq m/ um)	Mag 0 Gathered Power (W/um)	Mag 0 Gathered Power (phot./sec/ um)	Mag 0 Gathered Power (phot./sec)			Single Magnitude Energy Differential		INT value of Pixels per Airy Disc	INT Value of Pixels Per Seeing Limited Spot	Diffraction Limited Pixels per Site Seeing Spot		Sky Noise (ph/ pixel/ sec)		Dark Current Noise (PE / second)
0.000000039	3.7522E-10	2.345E+09	1.173E+09			2.5		1	0	1		0		200

		SIGNAL TO NOISE RATIO (Fstar/ Fsky) *						PHOTONS PER PIXEL WELL PER EXPOSURE (ignores gain)						EM Gain Electrons Per Pixel Per Exposure (Max Gain)					
	Exposure Time	*0.01*	*0.1*	*1*	*10*	*100*	*1000*	*0.01*	*0.1*	*1*	*10*	*100*	*1000*	*0.01*	*0.1*	*1*	*10*	*100*	*1000*
Star Mag	0	5.14E+06	1.63E+07	5.14E+07	1.63E+08	5.14E+08	1.63E+09	1.17E+07	1.17E+08	1.17E+09	1.17E+10	1.17E+11	1.17E+12	1.17E+10	1.17257E+11	1.17E+12	1.17E+13	1.17E+14	1.17E+15
Star Mag	1	2.06E+06	6.50E+06	2.06E+07	6.50E+07	2.06E+08	6.50E+08	4.69E+06	4.69E+07	4.69E+08	4.69E+09	4.69E+10	4.69E+11	4.69E+09	46902996570	4.69E+11	4.69E+12	4.69E+13	4.69E+14
Star Mag	2	8.22E+05	2.60E+06	8.22E+06	2.60E+07	8.22E+07	2.60E+08	1.88E+06	1.88E+07	1.88E+08	1.88E+09	1.88E+10	1.88E+11	1.88E+09	18761198628	1.88E+11	1.88E+12	1.88E+13	1.88E+14
Star Mag	3	3.29E+05	1.04E+06	3.29E+06	1.04E+07	3.29E+07	1.04E+08	7.50E+05	7.50E+06	7.50E+07	7.50E+08	7.50E+09	7.50E+10	7.5E+08	7504479451	7.5E+10	7.5E+11	7.5E+12	7.5E+13
Star Mag	4	1.32E+05	4.16E+05	1.32E+06	4.16E+06	1.32E+07	4.16E+07	3.00E+05	3.00E+06	3.00E+07	3.00E+08	3.00E+09	3.00E+10	3E+08	3001791781	3E+10	3E+11	3E+12	3E+13
Star Mag	5	5.26E+04	1.66E+05	5.26E+05	1.66E+06	5.26E+06	1.66E+07	1.20E+05	1.20E+06	1.20E+07	1.20E+08	1.20E+09	1.20E+10	1.2E+08	1200716712	1.2E+10	1.2E+11	1.2E+12	1.2E+13
Star Mag	6	2.11E+04	6.66E+04	2.11E+05	6.66E+05	2.11E+06	6.66E+06	4.80E+04	4.80E+05	4.80E+06	4.80E+07	4.80E+08	4.80E+09	48028668	480286684.9	4.8E+09	4.8E+10	4.8E+11	4.8E+12
Star Mag	7	8.42E+03	2.66E+04	8.42E+04	2.66E+05	8.42E+05	2.66E+06	1.92E+04	1.92E+05	1.92E+06	1.92E+07	1.92E+08	1.92E+09	19211467	192114674	1.92E+09	1.92E+10	1.92E+11	1.92E+12
Star Mag	8	3.37E+03	1.07E+04	3.37E+04	1.07E+05	3.37E+05	1.07E+06	7.68E+03	7.68E+04	7.68E+05	7.68E+06	7.68E+07	7.68E+08	7684587	76845869.58	7.68E+08	7.68E+09	7.68E+10	7.68E+11
Star Mag	9	1.35E+03	4.26E+03	1.35E+04	4.26E+04	1.35E+05	4.26E+05	3.07E+03	3.07E+04	3.07E+05	3.07E+06	3.07E+07	3.07E+08	3073835	30738347.83	3.07E+08	3.07E+09	3.07E+10	3.07E+11
Star Mag	10	5.39E+02	1.70E+03	5.39E+03	1.70E+04	5.39E+04	1.70E+05	1.23E+03	1.23E+04	1.23E+05	1.23E+06	1.23E+07	1.23E+08	1229534	12295339.13	1.23E+08	1.23E+09	1.23E+10	1.23E+11
Star Mag	11	2.16E+02	6.82E+02	2.16E+03	6.82E+03	2.16E+04	6.82E+04	4.92E+02	4.92E+03	4.92E+04	4.92E+05	4.92E+06	4.92E+07	491813.6	4918135.653	49181357	4.92E+08	4.92E+09	4.92E+10
Star Mag	12	8.62E+01	2.73E+02	8.62E+02	2.73E+03	8.62E+03	2.73E+04	1.97E+02	1.97E+03	1.97E+04	1.97E+05	1.97E+06	1.97E+07	196725.4	1967254.261	19672543	1.97E+08	1.97E+09	1.97E+10
Star Mag	13	3.45E+01	1.09E+02	3.45E+02	1.09E+03	3.45E+03	1.09E+04	7.87E+01	7.87E+02	7.87E+03	7.87E+04	7.87E+05	7.87E+06	78690.17	786901.7045	7869017	78690170	7.87E+08	7.87E+09
Star Mag	14	1.38E+01	4.36E+01	1.38E+02	4.36E+02	1.38E+03	4.36E+03	3.15E+01	3.15E+02	3.15E+03	3.15E+04	3.15E+05	3.15E+06	31476.07	314760.6818	3147607	31476068	3.15E+08	3.15E+09
Star Mag	15	5.52E+00	1.75E+01	5.52E+01	1.75E+02	5.52E+02	1.75E+03	1.26E+01	1.26E+02	1.26E+03	1.26E+04	1.26E+05	1.26E+06	12590.43	125904.2727	1259043	12590427	1.26E+08	1.26E+09
Star Mag	16	2.21E+00	6.98E+00	2.21E+01	6.98E+01	2.21E+02	6.98E+02	5.04E+00	5.04E+01	5.04E+02	5.04E+03	5.04E+04	5.04E+05	5036.171	50361.70909	503617.1	5036171	50361709	5.04E+08
Star Mag	17	8.83E-01	2.79E+00	8.83E+00	2.79E+01	8.83E+01	2.79E+02	2.01E+00	2.01E+01	2.01E+02	2.01E+03	2.01E+04	2.01E+05	2014.468	20144.68364	201446.8	2014468	20144684	2.01E+08
Star Mag	18	3.53E-01	1.12E+00	3.53E+00	1.12E+01	3.53E+01	1.12E+02	8.06E-01	8.06E+00	8.06E+01	8.06E+02	8.06E+03	8.06E+04	805.7873	8057.873454	80578.73	805787.3	8057873	80578735
Star Mag	19	1.41E-01	4.47E-01	1.41E+00	4.47E+00	1.41E+01	4.47E+01	3.22E-01	3.22E+00	3.22E+01	3.22E+02	3.22E+03	3.22E+04	322.3149	3223.149382	32231.49	322314.9	3223149	32231494
Star Mag	20	5.65E-02	1.79E-01	5.65E-01	1.79E+00	5.65E+00	1.79E+01	1.29E-01	1.29E+00	1.29E+01	1.29E+02	1.29E+03	1.29E+04	128.926	1289.259753	12892.6	128926	1289260	12892598
Star Mag	21	2.26E-02	7.15E-02	2.26E-01	7.15E-01	2.26E+00	7.15E+00	5.16E-02	5.16E-01	5.16E+00	5.16E+01	5.16E+02	5.16E+03	51.57039	515.7039011	5157.039	51570.39	515703.9	5157039

below noise floor or oversaturated and bleeding
marginal signal level pixel
within visible well capacity

* Ignores star flux as a source of shot noise: irrelevant to limiting sensitivity analysis

Fig 2: EOSSS standard tool for expected limiting sensitivity based on FoV

In Fig 2 above, the selected FoV and pixel size data entered in the Fig 1 data sheet are referenced to derive the signal to noise ratio (SNR) for various exposure scenarios. For various visual magnitude objects, the SNR is displayed and the Conditional Formatting facility is used to show useable ranges. This allows designers to see at a glance whether they have selected the best pixel scale for their purpose when considering tracking of orbiting objects.

The EOS design was based on a specification for maximum practical field of view, using the Andor Ixon EMCCD product with 512x512 pixel array, each pixel being 13 microns on a side. Plugging this into the tool, it became evident that detection efficiency is optimum for effective focal ratios smaller than f2.0, and this became a driving parameter for the optical design.

Within the range of focal ratios where neither sky noise nor oversampling dominate the performance limits, it was decided to accept more sky noise by designing for the smallest focal ratio achievable. Tracking of objects is slightly affected by the effects of moonlight sky noise, but the imager is able to use its large sky area per pixel for another operational regime: staring acquisition. In cases where no orbital information is available, the performance limitation becomes something new, which is the “pixel crossing time”. In this regime, the exposure period becomes irrelevant compared to the relatively short periods in which photons collect within a single pixel well.

Optical Design Issues

Early experience allowed the EOSSS designers to say with certainty that f2.0 is already a difficult challenge, with off axis performance suffering from coma. In fact, the earliest designs were f2.0 Celestron OTAs with Fastar/ Ultrastar ™ corrector optics used in a prime focus configuration, and this concept was used for the latest imager design. EOSSS CEO Craig Smith demonstrated that with the prime focus design, opto-mechanical tolerancing is more manageable.

The problem areas now were cost of correction optics and mechanical stability within a tight tolerance budget. At focal ratios faster than f2.0, the separation and decentre tolerances of the optical elements drops below 50 microns. This is a constant challenge for all wide field imaging designs, and the cost of fabrications becomes very large when dealing with stable materials such as INVAR 36. Weight of components also becomes an issue.

The mounting material issue was finally resolved by selecting sealed Carbon Fibre Reinforced Plastic (CFRP), which is light and has low thermal expansion coefficient. By sealing with flowcoat as in boat design, the diffusion of local humidity can be limited, and the material will have maximum resistance to effects of both temperature and water vapour pressures. This has proven to be good choice, limiting the structural assembly mass to ~40kg.

With optical handling stability solved, the optical design was performed using a unique approach involving maximum use of spherical polished elements. While this created the possibility of very high powered inexpensive elements, it did nothing to resolve the off axis aberrations which dominate the optical performance of fast imaging systems. The primary attraction of spherical elements is that their off-axis aberrations are limited to large amounts of spherical aberration. With minmal coma. This single form of residual aberration can be corrected with minimal use of aspheric elements.

After several weeks of effort the EOSSS optical designer created a design with minimum use of aspheric components, but with effective focal ratio of f0.75. This created a very large FoV capability even with the modest image plane sizes of the Andor detector, but with acceptable off axis performance in coma and spherical aberration. Using the CFRP housing material, the required stability of despace and decenter to within 20 microns can be achieved, such that focus tweaking is only necessary in seasonal changes of ambient temperature.

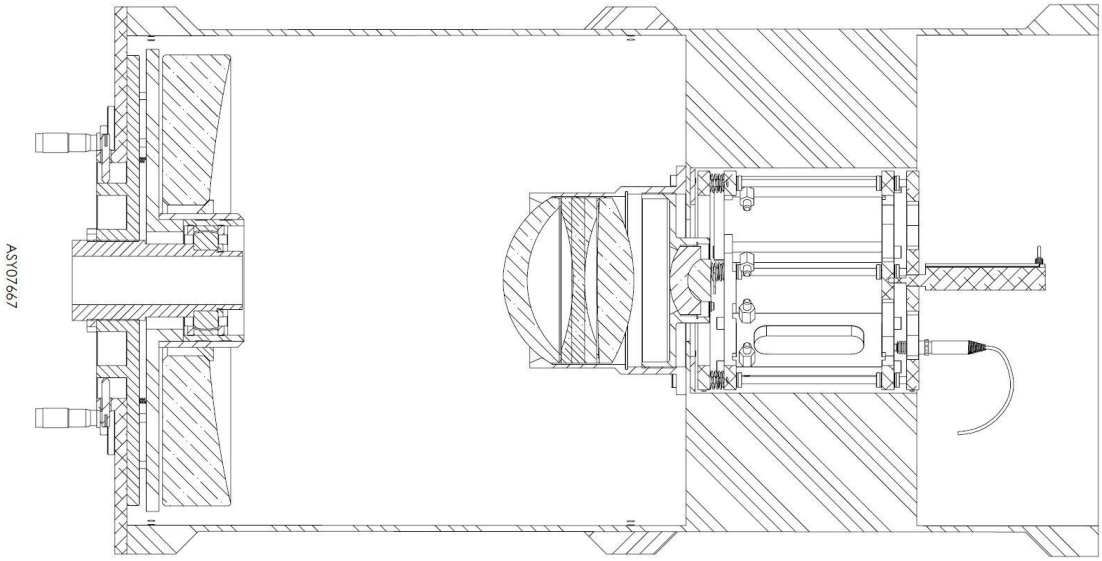

Fig 3: Cross section of the wide field imager

The Andor detector is mounted completely within the optical tube assembly, protecting it from external shocks. Water cooling is provided to limit the effects of warmed air from the detector electronics. By mounting the detector on linear bearings, a micrometer screw is used with a servomotor to control focus from a simple CAN circuit. The decentre of the detector is tightly controlled by the linear bearings, which provides boresight stability when tilting the instrument.

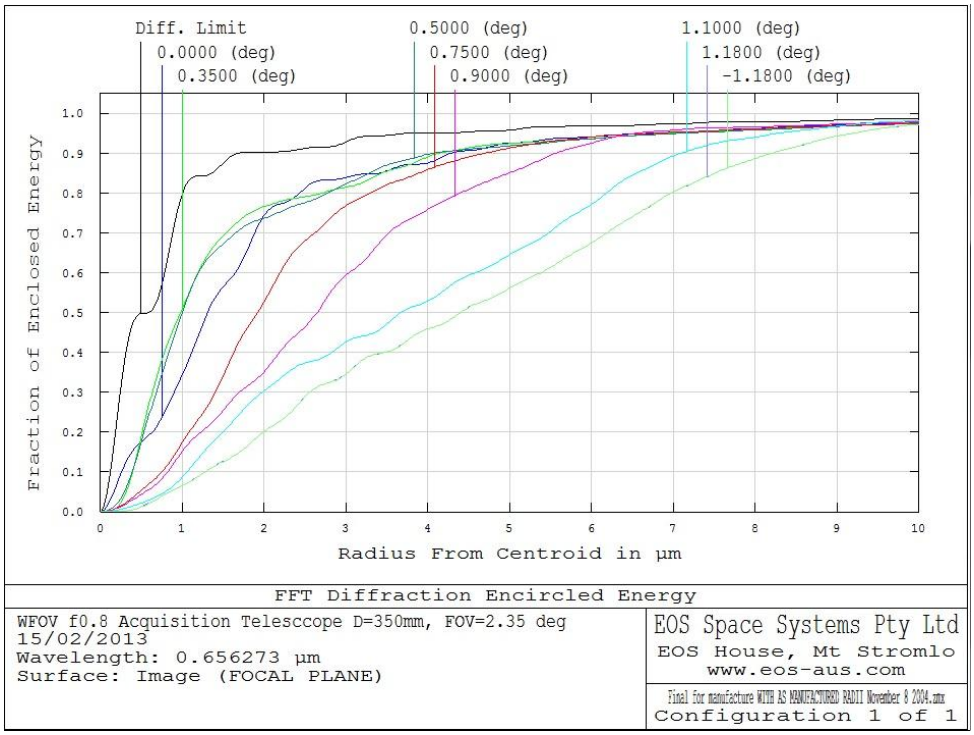

Fig 4: ZEMAX analysis of the wide field imager design

		SIGNAL TO NOISE RATIO (Fstar/ Fsky) *					
	Exposure Time (Sec)	*0.01*	*0.1*	*1*	*10*	*100*	*1000*
Star Mag	0	2.34E+06	7.39E+06	2.34E+07	7.39E+07	2.34E+08	7.39E+08
Star Mag	1	9.34E+05	2.96E+06	9.34E+06	2.96E+07	9.34E+07	2.96E+08
Star Mag	2	3.74E+05	1.18E+06	3.74E+06	1.18E+07	3.74E+07	1.18E+08
Star Mag	3	1.50E+05	4.73E+05	1.50E+06	4.73E+06	1.50E+07	4.73E+07
Star Mag	4	5.98E+04	1.89E+05	5.98E+05	1.89E+06	5.98E+06	1.89E+07
Star Mag	5	2.39E+04	7.57E+04	2.39E+05	7.57E+05	2.39E+06	7.57E+06
Star Mag	6	9.57E+03	3.03E+04	9.57E+04	3.03E+05	9.57E+05	3.03E+06
Star Mag	7	3.83E+03	1.21E+04	3.83E+04	1.21E+05	3.83E+05	1.21E+06
Star Mag	8	1.53E+03	4.84E+03	1.53E+04	4.84E+04	1.53E+05	4.84E+05
Star Mag	9	6.12E+02	1.94E+03	6.12E+03	1.94E+04	6.12E+04	1.94E+05
Star Mag	10	2.45E+02	7.75E+02	2.45E+03	7.75E+03	2.45E+04	7.75E+04
Star Mag	11	9.80E+01	3.10E+02	9.80E+02	3.10E+03	9.80E+03	3.10E+04
Star Mag	12	3.92E+01	1.24E+02	3.92E+02	1.24E+03	3.92E+03	1.24E+04
Star Mag	13	1.57E+01	4.96E+01	1.57E+02	4.96E+02	1.57E+03	4.96E+03
Star Mag	14	6.27E+00	1.98E+01	6.27E+01	1.98E+02	6.27E+02	1.98E+03
Star Mag	15	2.51E+00	7.93E+00	2.51E+01	7.93E+01	2.51E+02	7.93E+02
Star Mag	16	1.00E+00	3.17E+00	1.00E+01	3.17E+01	1.00E+02	3.17E+02
Star Mag	17	4.01E-01	1.27E+00	4.01E+00	1.27E+01	4.01E+01	1.27E+02
Star Mag	18	1.61E-01	5.08E-01	1.61E+00	5.08E+00	1.61E+01	5.08E+01
Star Mag	19	6.42E-02	2.03E-01	6.42E-01	2.03E+00	6.42E+00	2.03E+01
Star Mag	20	2.57E-02	8.12E-02	2.57E-01	8.12E-01	2.57E+00	8.12E+00
Star Mag	21	1.03E-02	3.25E-02	1.03E-01	3.25E-01	1.03E+00	3.25E+00

Fig 5: Excel analysis tool – SNR performance

Installation and Practical Performance

The entire assembly weighs ~50kg, and may be mounted onto the optical tube assembly of a 1m or larger telescope, if such "piggyback" mounting has been allowed for in the host telescope design. EOS Space Systems has mounted the imager to its 1.8m telescope at Mount Stromlo, currently on loan from the US Naval Observatory.

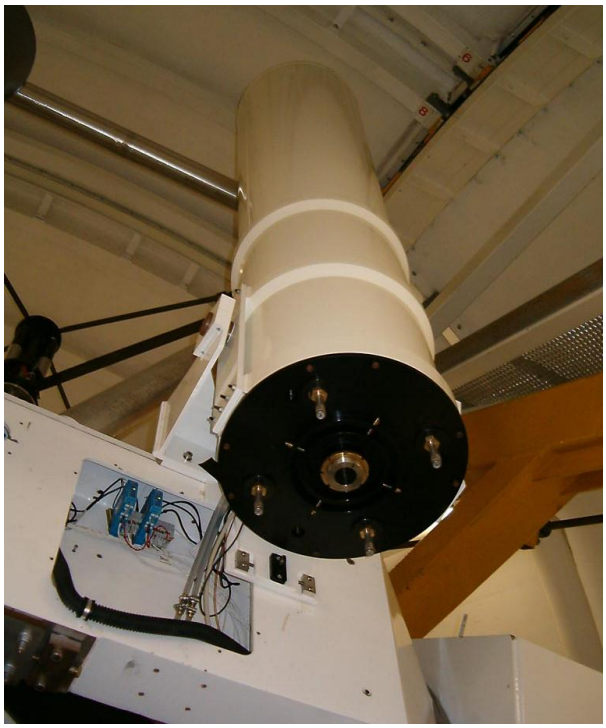

Fig 6: Wide field imager installed

As mounted, the boresight flexure is not identical to that of the main telescope, but this difference is mapped in software with elevation, and the main telescope boresight is represented by a green cross hair on the wide field image. This allows the imager to locate an object of interest and 'transfer' it to the main telescope autoguider. These are referred to as "capture" and "lock" modes of system operation.

As Fig 7 below shows, the sensitivity is perfectly adequate for small objects, but the star background can become a problem.

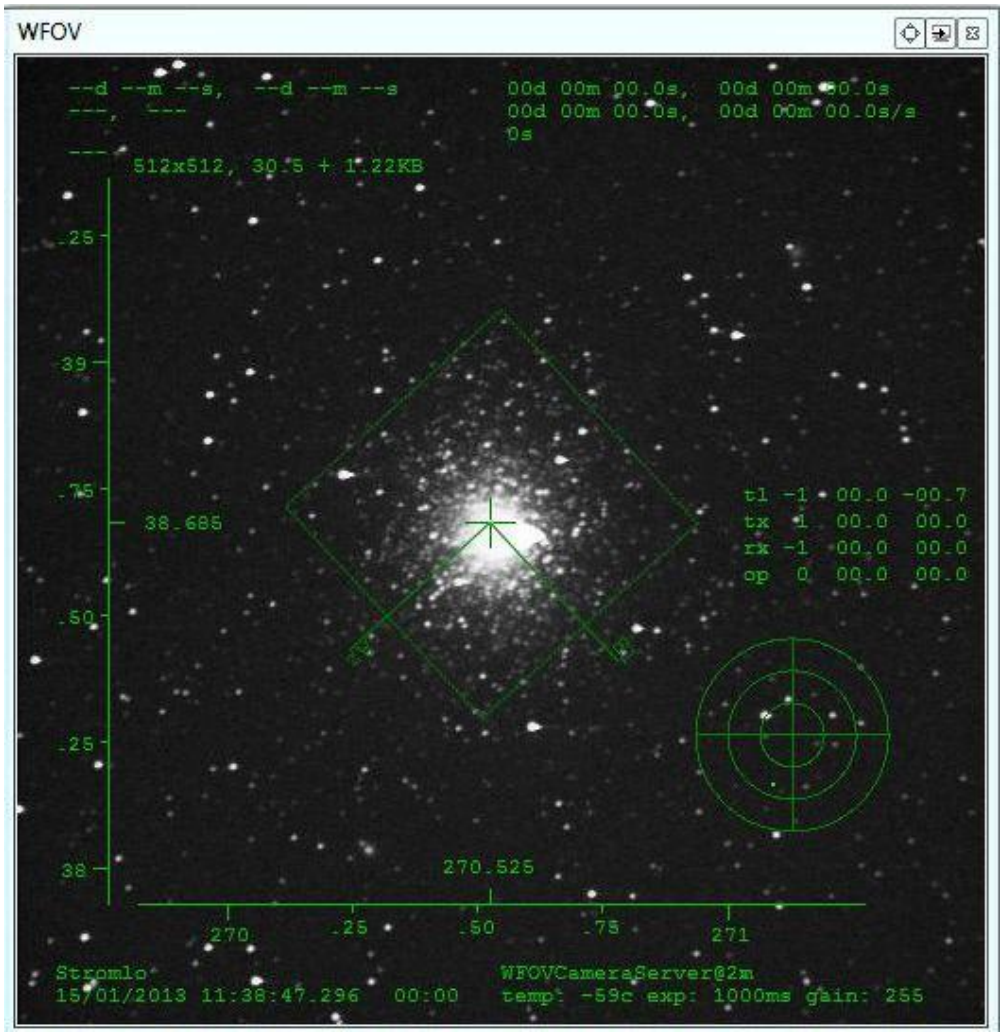

Fig 7: Globular cluster as an extreme example of background clutter

Of relevance in Fig 7 is the exposure period of 1 second. In moonlight conditions at Mount Stromlo (elevation 800m), the sky noise begins to dominate at 2 second exposures. This is an example of the performance tradeoff between FoV and limiting sensitivity when using f0.75 instead of f2.0, as described above. The background is clearly no longer black, but a dark gray at 1 second exposure. In this image, the dimmest objects are likely to be only visual magnitude 16, with software detection possible at magnitude 17. In dark sky conditions the limiting visual magnitude can extend to magnitude 18, but the star clutter problem for tracking orbiting bodies becomes very challenging. At 2 second exposures, the entire field can be a pattern of streaks, obscuring the small object of interest.

Processing Enhancements in Real Time

Software development has been successful in improving signal to noise ratios on objects tracked with a strong star background. Three primary filters are used frequently to enhance the object of interest when detecting it. Keeping in mind that recognition is not a requirement, the non linear effects of high detector gain can be used to advantage here.

The images below are typical of the beneficial effects of real time electronic filtering for faint objects. Camera maximum and minimum levels are used first, for autoscaling contrast enhancement.

Fig 8: Raw image after camera optimisation of levels, then with streak removal, and with temporal filtering

It is clear from the images that streak removal works well unless streak overlap occurs within one frame, but that pixel by pixel temporal comparison filtering works well to enhance persistent objects and remove transient pixel exposures.

The final type of filter applied identifies contiguous image elements with a significantly lower aspect ratio than their neighbours. This is known as "blob detection" and isolates tracked objects as having rounder shape than other image elements in a frame. In the right hand side of fig 8 below, yellow objects are blobs rather than streaks, red is the roundest aspect ratio blob, and green pixels overlaid on the red are used for the relevant centroid.

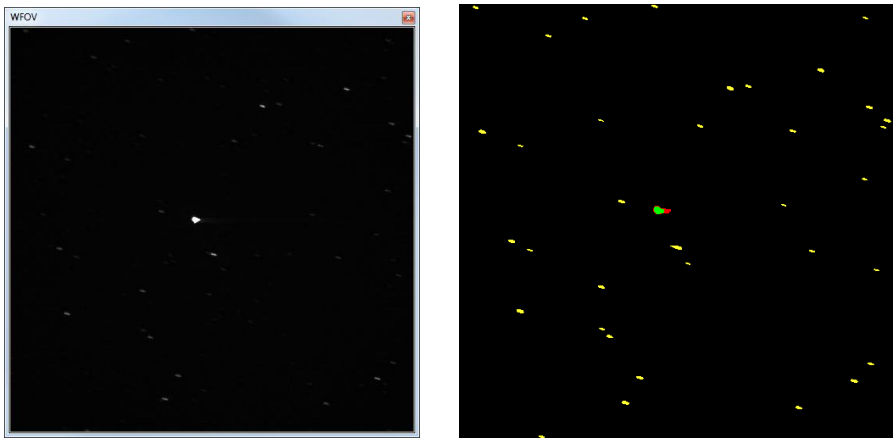

Fig 9: Aspect ratio filter for "blob detection"

References